

1.5-Mbit/s direct readout of line-and-space patterns using a scanning near-field optical microscopy probe slider with air-bearing control

F. Issiki,^{a)} K. Ito, K. Etoh, and S. Hosaka

Central Research Laboratory (CRL), Hitachi Ltd., 1-280 Higashi-koigakubo, Kokubunji-shi, Tokyo 185-8601, Japan

(Received 22 October 1999; accepted for publication 16 December 1999)

We have demonstrated 1.5-Mbit/s signal readout of a 0.25 μm line-and-space (L&S) pattern on a rotating disk by using a scanning near-field optical microscopy (SNOM) probe slider with air-bearing control. The light transmittance of the probe was greatly increased through direct irradiation of a focused light to a pyramidal probe tip. The bit rate of the signal was enhanced by two orders of magnitude compared to that of existing SNOM systems that use a tapered-fiber probe. The signal contrast, signal-to-noise ratio, and carrier-to-noise ratio for the 0.25 μm L&S pattern were 19%, 17 dB, and 37 dB, respectively. The estimated resolution limit of the probe corresponded to a L&S width of ~ 130 nm. © 2000 American Institute of Physics. [S0003-6951(00)02307-X]

Recording density is the central concern when we develop data-storage systems for multimedia applications. For optical disk recording, vast efforts have been devoted to reducing the beam spot size to increase the bit areal density and storage capacity. The use of blue light with shorter wavelengths,^{1,2} a solid immersion lens (SIL),^{3,4} scanning near-field optical microscopy (SNOM) with tapered-fiber probes,⁵⁻⁸ super-resolution techniques,^{9,10} and high-refractive-index materials² have all been demonstrated.

An SNOM-based system has an advantage in that it can achieve a higher recording density than that achieved through other approaches because it can go beyond the optical limits determined by the light wavelength and a material's refractive index. The application of SNOM to information storage has reduced the mark size, and a pit diameter of 60 nm and a clear readout of the bit signal has been achieved in phase-change recording using a GeSbTe film with a tapered-fiber probe.¹¹ The problem, in terms of practical application to an actual information storage system, is that the readout speed remains too low. The readout speed is determined by the light transmittance of the SNOM probe. In a typical tapered-fiber probe with a resolution of about 100 nm, the transmittance is below 10^{-4} and the readout speed is limited to about 10 kbit per second (kbps).¹² The transmittance will have to be increased by at least two orders of magnitude to achieve a bit rate of more than 1 Mbps, which is equivalent to the bit rate in a practical optical disk system such as a compact-disk (CD) player.

We have developed a type of probe slider, an SNOM-based optical disk head that enables a much higher bit rate than existing fiber-based SNOM probes and a higher recording density than an SIL-based system. The light transmittance was increased in combination with direct irradiation of focused light to the probe-top aperture. Here, we describe the structure of the probe slider and demonstrate its readout property. We estimated the resolution of the slider probe through contrast analysis of the readout signal from line-and-space (L&S) patterns. The direct readout signal was mea-

sured to demonstrate the potential of the system. Noise properties of the readout signal, such as the signal-to-noise (S/N) and carrier-to-noise (C/N) ratios, were also evaluated.

We fabricated the SNOM probe slider by using photolithography and a focused ion beam (FIB) cutting technique. The structure of the slider is shown in Fig. 1(a). Slider pads were formed on a 0.6-mm-thick SiO_2 wafer by the usual lithography technique with reactive ion etching, then the wafer was cut into 5 mm \times 5 mm slider chips. The size of the pads was 50 μm \times 50 μm , and the pads were spaced 30 μm apart. The SNOM tip was located at the center between four pads. This four-pad structure was used to reduce the flight height during the disk rotation because the resolution of the

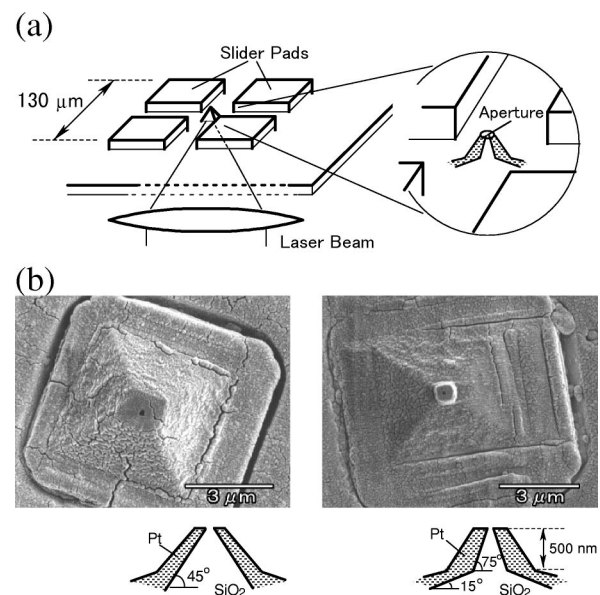


FIG. 1. (a) Structure of single- and double-tapered SNOM probes with sliding pads. The probe tip is located in the center between four pads that are each 50 μm square. (b) SEM images of the probe tip. The angle of the tapered tip was 45° for the single-tapered probe, and 15° and 75° for the double-tapered probe. Total chip size was 5 mm \times 5 mm. The light was directly illuminated from the backside of the chip and focused onto the aperture at the probe tip.

^{a)}Electronic mail: fisisaki@crl.hitachi.co.jp

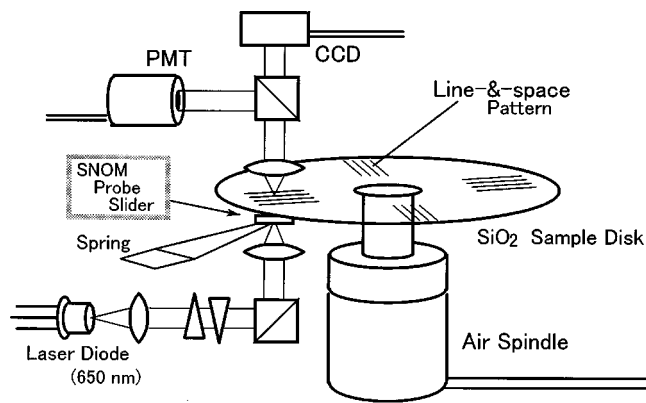


FIG. 2. Optical setup for line-and-space (L&S) pattern readout. The light source was a 650 nm laser diode (LD). Typical light power of the LD was 25 mW. The SNOM probe slider was set just below the sample disk, on which tungsten L&S patterns were drawn. The transmitted light was collected by an objective lens and detected with a photomultiplier (PMT) and charge-coupled device (CCD).

SNOM probe is more sensitive than the resolution of the SIL-based system to the distance from the disk surface. Typical scanning electron microscope (SEM) images of these probe tips are shown in Fig. 1(b). We fabricated two types of pyramidal-tip probes: the first one was a single-tapered probe with a slope angle of 45° , and the second was a double-tapered probe with slope angles of 15° and 75° . The total height of the probe tip was typically $2 \mu\text{m}$ and the height of the second taper in the double-tapered probe was 500 nm. After evaporation of a Pt shading film that was 200–500 nm thick, the top of the probe tip was sliced using FIB to form the aperture. The typical aperture size and the transmittance of the probes were, respectively, $150 \pm 10 \text{ nm}$ and 0.5% for the single-tapered probe, and $50 \pm 10 \text{ nm}$ and 0.14% for the double-tapered probe. The aperture sizes were determined from SEM images. The transmittance of the probe was measured in a far-field configuration using 660 nm laser light focused to a $3 \mu\text{m}$ spot. These increases in the aperture transmittance, compared to the fiber-based SNOM probes, were mainly due to improved light intensity near the probe-tip aperture. Our results suggest that the low light efficiency of the usual tapered-fiber probe is due to the propagation loss of the light caused by reflection in the tapered region of the fiber.¹³

Figure 2 shows the optical setup of the measurement system for the L&S pattern signal readout. The slider chip was set just below a sample disk on which tungsten L&S patterns with widths of 1.0, 0.5 and $0.25 \mu\text{m}$ were drawn. (The $1 \mu\text{m}$ L&S pattern consisted of a $1 \mu\text{m}$ line and a $1 \mu\text{m}$ space, so the pitch was $2 \mu\text{m}$. The pitches of the other L&S patterns are doubled in the same manner.) The chip was supported by a leaf-spring suspension. The angle of the chip was carefully adjusted so that the chip was parallel to the disk surface to enable air bearing with the disk rotation. The sample disk was rotated using an air spindle with servo-speed control. The light source was a 650-nm-wavelength laser diode with a total power of 35 mW. After collimation and beam shaping, the laser light was focused directly onto the probe tip from the backside of the slider chip with an objective lens whose numerical aperture (NA) was 0.6. Transmitted light was collected from the other side of the

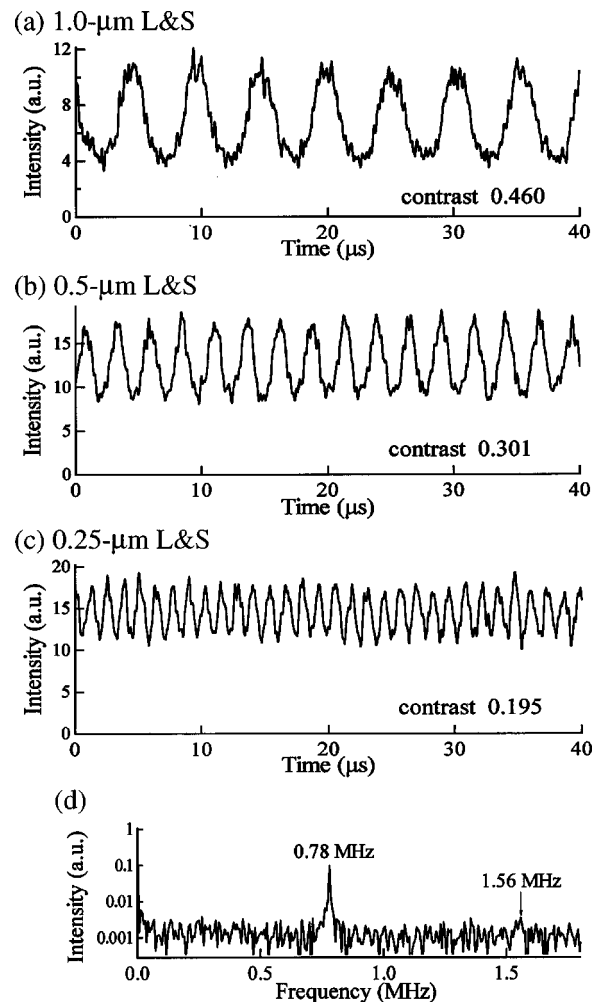


FIG. 3. Readout signal from L&S patterns of (a) $1 \mu\text{m}$, (b) $0.5 \mu\text{m}$, and (c) $0.25 \mu\text{m}$ widths obtained using a double-tapered SNOM probe at a rotation speed of 150 rpm (linear velocity 0.38 m/s). The frequency spectra of the $0.25 \mu\text{m}$ L&S signal is also shown in (d). The maximum frequency was 0.78 MHz. The doubled-frequency peak at 1.56 MHz suggests the potential resolution of the probe will enable reading of patterns with a mark size or L&S width of 125 nm.

sample disk by a second objective lens ($\text{NA}=0.8$) and sent to a photomultiplier and an image detector with a charge-coupled device (CCD). This CCD image detector was set to check the optical setup during the readout measurement of the L&S pattern. The bandwidth (-3 dB) of the photomultiplier was 4 MHz.

Figures 3(a) to 3(c) show the readout signals from the 1.0, 0.5, and $0.25 \mu\text{m}$ L&S patterns that were obtained using the double-tapered probe at a rotation speed of 150 rpm with a linear velocity of 0.38 m/s . Figure 3(d) shows the frequency spectrum of the $0.25 \mu\text{m}$ L&S pattern signal. The signal was not equalized. The contrast of the signals was over 19% even for $0.25 \mu\text{m}$ L&S pattern which had a signal frequency of 0.78 MHz ($=f_c$). This frequency agrees with the value calculated from the pattern width and the disk linear velocity. The C/N ratio was 37 dB (band width 10 kHz). The S/N ratio was 17 dB in the range of $0.1 f_c \sim 1.5 f_c$ with an equalization, which is high enough for direct bit readout with nonreturn-to-zero inverted (NRZI) modulation. The bit rate of the signal was 1.56 Mbps, twice the frequency. This value is fairly close to the standard data bit rate of a CD (2.03 Mbps).

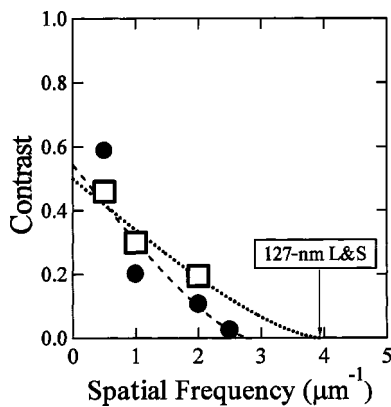


FIG. 4. Contrast plots of the L&S-pattern readout signal. The circles and squares show the contrast for the single- and double-tapered SNOM probes, respectively. The respective estimated cut-off frequencies of the probes corresponded to L&S pattern of the widths of 177 and 127 nm.

Figure 4 shows the contrast plots of the readout signals against the spatial frequency of the L&S patterns for the single- and double-tapered probes. The dotted lines in Fig. 4 show the fitted modulation transfer function (MTF) that is commonly used for optics in an incoherent system.¹⁴ This MTF is written as $M(\omega) = A[2 \arccos(B\omega/2) - \sin\{2 \arccos(B\omega/2)\}]/\pi$, where ω is the spatial frequency normalized by the effective spot size NA/λ , A and B are fitting constants. We fitted the MTF on a logarithmic contrast scale to emphasize its roll-off property. The optical cut-off frequency, at which the $M(\omega)$ reaches zero, was estimated from the fitted MTF to be $2.82 \mu\text{m}^{-1}$ for the single-tapered probe and $3.94 \mu\text{m}^{-1}$ for the double-tapered probe. These spatial frequencies correspond to L&S pattern widths of 177 and 127 nm, respectively. These values are consistent with the existence of multiple-frequency peaks in the frequency spectra. For the single-tapered probe, multiple-frequency peaks that exist up to 0.5 MHz at a linear velocity of 0.17 m/s correspond with the spatial frequency of a 170 nm L&S pattern, although these frequency spectra are not shown here. For the double-tapered probe, the faint existence of a doubled frequency peak at 1.56 MHz in Fig. 3(d) corresponds to the spatial frequency of a 125 nm L&S pattern. The double-tapered probe probably has a resolution sufficient to read a narrow L&S pattern with a width of less than 130 nm. This size roughly corresponds with the readout limit of the mark size in pit-pattern readout. The effective beam spot size was estimated to be about $0.26 \mu\text{m}$ ($130 \text{ nm} \times 2$), which is smaller than the previously reported spot sizes of 0.36 and $0.33 \mu\text{m}$ in an SIL-based system.^{3,4} Our cut-off frequency of $3.9 \mu\text{m}^{-1}$ is also higher than the reported $3.3 \mu\text{m}^{-1}$ cut-off frequency of an SIL-based optical head using 532 nm laser light.⁴ The resolution of the SNOM-based probe can be further improved if we can reduce the air gap between the probe tip and the disk surface, since this system's resolution is not limited by the light wavelength nor the refractive index of the materials, because the aperture size has already been reduced to $\sim 50 \text{ nm}$. We roughly estimated the air gap between the aperture and the disk surface to be $\sim 100 \text{ nm}$ from the sliced height of the tip apex ($50 \text{ nm}/2/\cos 75^\circ \approx 100 \text{ nm}$). This air gap seems to extend the effective beam spot size, and thus degrade the potential higher

resolution of the SNOM probe. (We estimated the flight height of this slider pad to be $\leq 6 \text{ nm}$ at this disk linear velocity using an air bearing simulator that solves the generalized Reynolds equation.¹⁵) We will continue our work to reduce the length of this air gap to about the same size as the aperture. Compared to a super-resolution-based readout system,^{9,10} this SNOM-based system has superior noise properties, such as its C/N ratio, because it is not susceptible to time-dependent fluctuation of the aperture size with grain crystallization in the super-resolution layer. (This is the dominant noise source in the current super-resolution-based system.) Our bit rate of 1.5 Mbps is now comparable to SIL-based magneto-optical disk readout at bit rates of 3.3 (Ref. 3) and 8.0 Mbps.⁴ The aperture transmittance in our SNOM-based system can be increased by one order of magnitude through combination with plasmon propagation effects if we change the shading metal source from Pt to Au.¹² Therefore, we expect to achieve the same bit rate with the SNOM-based probe head as those in current SIL-based systems.

In summary, we have demonstrated fast readout of a clear bit signal from a rotating disk using an SNOM-based probe slider with air-bearing control. The light transmittance of the probe was enhanced by two orders of magnitude through direct irradiation of focused laser light onto the probe tip. With the higher transmittance of the probe, the signal bit rate was increased to over 1.5 Mbps, which is two orders of magnitude higher than existing fiber-based SNOM systems. The estimated cut-off frequency of the probe was over $3.9 \mu\text{m}^{-1}$, so the readout limit of L&S pattern width or mark size corresponded to 130 nm.

The authors thank Masashi Kiguch in HARL, Hirokazu Matsubara in CRL, Yasuhiro Ito in Hitachi Metals, and Masayoshi Ishibashi in HARL for their valuable discussions. They also thank Midori Kato in HARL, Takeshi Shimano and Katsura Etoh in CRL, and Iwao Yamazaki in Hitachi Science Systems, for their technical support.

¹J. W. Kozlovsky, A. G. Dewey, A. Juliana, J. E. Hurst, M. R. Latta, D. A. Page, R. N. Payne, and H. Werlich, *Proc. SPIE* **1663**, 410 (1992).

²C. J. Robinson, R. N. Payne, and A. E. Bell, *J. Appl. Phys.* **64**, 4646 (1988).

³B. D. Terris, H. J. Mamin, and D. Rugar, *Appl. Phys. Lett.* **68**, 141 (1996); **65**, 388 (1994).

⁴I. Ichimura, S. Hayashi, and G. S. Kino, *Appl. Opt.* **36**, 4339 (1997).

⁵S. Hosaka, T. Shintani, M. Miyamoto, and A. Kikukawa, *J. Appl. Phys.* **79**, 8082 (1996).

⁶C. Durkan, I. V. Shvets, and J. C. Lodder, *Appl. Phys. Lett.* **70**, 1323 (1997); *J. Appl. Phys.* **81**, 5019 (1997).

⁷D. P. Tsai and W. R. Guo, *J. Vac. Sci. Technol. A* **15**, 1442 (1997).

⁸E. Betzig, M. Isaacson, and A. Lewis, *Appl. Phys. Lett.* **51**, 2088 (1987).

⁹T. Shintani, M. Terao, H. Yamamoto, and T. Naito, *Jpn. J. Appl. Phys., Part 1* **38**, 1656 (1999).

¹⁰J. Tominaga, T. Nakano, and N. Atoda, *Appl. Phys. Lett.* **73**, 2078 (1998); J. Tominaga and N. Atoda, *Technical Digest of Joint ISOM/ODS '99*, Koloa, Hawaii, July, 1999, p. 375.

¹¹S. Hosaka, A. Kikukawa, H. Koyanagi, T. Shintani, M. Miyamoto, K. Nakamura, and K. Etoh, *Nanotechnology* **8**, A58 (1997).

¹²K. Ito, A. Kikukawa, and S. Hosaka, *Technical Digest of ISOM '98*, Tsukuba, Japan, October, 1998, p. 154.

¹³L. Novotny, D. W. Pohl, and B. Hecht, *Opt. Lett.* **20**, 970 (1995); *Ultra-microscopy* **61**, 1 (1996).

¹⁴Read-out of Optical Discs (J. Braat), *Principles of Optical Disk Systems*, edited by E. R. Pike (Adam Hilger, Bristol, 1985), p. 14.

¹⁵E. Cha and D. B. Bogy, *ASME J. Tribol.* **117**, 36 (1995).